INTERNATIONAL JOURNAL OF
NUMERICAL ANALYSIS AND MODELING
Volume 11, Number 2, Pages 400–411

GEOMETRIC MULTIGRID METHODS ON STRUCTURED TRIANGULAR GRIDS FOR INCOMPRESSIBLE NAVIER-STOKES EQUATIONS AT LOW REYNOLDS NUMBERS

F.J. GASPAR, C. RODRIGO, AND E. HEIDENREICH

(Communicated by J.L. Gracia)

This paper is dedicated to Francisco Lisbona on occasion of his 65th birthday

Abstract. The main purpose of this work is the efficient implementation of a multigrid algorithm for solving Navier-Stokes problems at low Reynolds numbers in different triangular geometries. In particular, a finite element formulation of the Navier-Stokes equations, using quadratic finite elements for the velocities and linear finite elements to approximate the pressure, is used to solve the problem of flow in a triangular cavity, driven by the uniform motion of one of its side walls. An appropriate multigrid method for this discretization of Navier-Stokes equations is designed, based on a Vanka type smoother. Moreover, the data structure used allows an efficient stencil-based implementation of the method, which permits us to perform simulations with a large number of unknowns with low memory consumption and a relatively low computational cost.

Key words. Multigrid methods, Navier-Stokes equations, Vanka smoother, Cavity problem

1. Introduction

One of the most important aspects in the numerical simulation of the Navier-Stokes equations is the efficient solution of the large sparse systems of equations arising from their discretization. This work is focused on an efficient implementation and the solution by geometric multigrid methods of the incompressible Navier-Stokes equations on structured triangular grids.

It is well-known that multigrid methods [2, 4, 8, 17] are among the fastest algorithms to solve large systems of equations, with small convergence factors which are independent of the space discretization parameter, and achieve optimal computational complexity of $\mathcal{O}(N)$, where N is the number of unknowns of the system. Geometric multigrid methods were initially developed for structured grids. However, in order to deal with relatively complex domains, an efficient implementation of this type of multigrid methods can be done on semi-structured triangular grids, see [6]. As a preliminary step towards this generalization, here we develop a geometric multigrid code suitable for efficiently solving this problem on a structured grid arising in a single triangular domain, which later will be part of the semi-structured grid.

An important step in the analysis of partial differential equations (PDE) problems using finite element methods is the construction of the large sparse matrix $\mathcal{A}$ corresponding to the system of discrete equations. The standard algorithm for computing matrix $\mathcal{A}$ is known as *assembly*, and consists of computing this matrix by iterating over the elements of the mesh and adding from each element of the triangulation the local contribution to the global matrix $\mathcal{A}$. Because of the size of this

Received by the editors October 30, 2012 and, in revised form, July 6, 2013.
2000 *Mathematics Subject Classification.* 65N55, 65F10.
This research has been partially supported by FEDER/MCYT Projects MTM2010-16917 and the DGA (Grupo consolidado PDIE)..

matrix, it is important to store it in an efficient way. However, the data structures needed to represent this type of sparse matrices can cause slowness in the code due to the use of indirect indexing to access the non-zero entries of the matrix. By working on structured grids, the necessary data structures are much more efficient and lead to better performance, due to the fact that explicit assembly of the global matrix is not necessary and that the matrix can be stored using stencils.

In this work, a stencil-based implementation of the Taylor-Hood element for the Navier-Stokes equations is presented, together with the design of an efficient geometric multigrid algorithm, based on a box-type smoother, to solve the large system of equations arising from this type of finite element discretization. More concretely, the outline of this work is as follows. In Section 2, the considered problem is presented, together with the linearization and the proposed finite element discretization. Section 2.1 is devoted to describe the stencil-based implementation of the Taylor-Hood element discretization of Navier-Stokes equations. Section 3 is focused on the design of a suitable geometric multigrid method, based on Vanka-type smoothers. Finally, in Section 4, the lid-driven recirculating flow in a triangular cavity is simulated, using the proposed multigrid solution procedure.

2. Finite element discretization of the Navier-Stokes equations

In this work we consider the Navier-Stokes equations governing a two-dimensional, steady, incompressible flow of constant fluid properties. These equations are written in primitive variables as

$$\begin{aligned} -\nu\Delta\mathbf{u} + (\mathbf{u}\cdot\nabla)\mathbf{u} + \nabla p &= \mathbf{0}, && \text{in } \Omega, \\ \operatorname{div}\mathbf{u} &= 0, && \text{in } \Omega, \\ \mathbf{u} &= \mathbf{g}, && \text{on } \Gamma = \partial\Omega, \end{aligned} \tag{1}$$

where $\mathbf{u} = (u, v)^t$ denotes the velocity vector, p is the pressure, and ν is the kinematic viscosity of the fluid. The Dirichlet boundary condition for the velocity is given by $\mathbf{g}$, which satisfies the following compatibility condition

$$\int_{\partial\Omega} \mathbf{g}\cdot\mathbf{n}\,\mathrm{d}\Gamma = 0, \tag{2}$$

where $\mathbf{n}$ is the outward direction normal to the boundary.

Nonlinear problem (1) is linearized using a fixed point iteration, that is, given a current iterate $(\mathbf{u}^n, p^n)$, in each nonlinear iteration step a problem of the following form has to be solved

$$\begin{aligned} -\nu\Delta\mathbf{u}^{n+1} + (\mathbf{u}^n\cdot\nabla)\mathbf{u}^{n+1} + \nabla p^{n+1} &= \mathbf{0}, && \text{in } \Omega, \\ \operatorname{div}\mathbf{u}^{n+1} &= 0, && \text{in } \Omega, \\ \mathbf{u}^{n+1} &= \mathbf{g}, && \text{on } \Gamma = \partial\Omega. \end{aligned} \tag{3}$$

Problem (3) is known in the literature as the Oseen problem. We are going to consider its discretization by finite element methods. For this purpose, let $\mathcal{T}_h$ be an admissible triangulation of the domain Ω, that is, Ω is decomposed into a set of triangles $\{K_i\}_{i=1}^N$ in the way that

$$\overline{\Omega} = \bigcup_{i=1}^{N} K_i,$$

and satisfying that the intersection $K_i \cap K_j$, for $i \neq j$, is either empty, a common vertex, or a common edge. Problem (3) is discretized using $P2-P1$ finite elements, where Pk is the space of piecewise polynomial continuous functions of degree k.

Thus, the velocity is represented on each triangular element by its values at six grid-points (the three vertices and the three midpoints of the edges of the triangle), and it is interpolated by using quadratic polynomials. The pressure is represented by the three nodes associated with the vertices, and it is interpolated by lineal polynomials. This pair of finite element spaces guarantees the inf-sup stability condition of Babuška-Brezzi, and thus, it ensures the unique solution of our discrete problem, see [3]. Moreover, since here we consider flow problems with low Reynolds numbers (e.g., less than 1000 for the 2D driven cavity, and less than 100 for the flow around a cylinder), it is not necessary to apply stabilization techniques regarding the convective term.
Thus, the linearization and the discretization of the incompressible Navier-Stokes equations lead to large saddle point problems of the form

$$\mathcal{A}\begin{pmatrix} u \\ p \end{pmatrix} = \begin{pmatrix} A & B \\ B^t & 0 \end{pmatrix}\begin{pmatrix} u \\ p \end{pmatrix} = \begin{pmatrix} f \\ g \end{pmatrix},$$

that must be solved at each iteration.

2.1. Stencil implementation. The purpose of this section is to present an efficient stencil-based implementation of the finite element method proposed to discretize the Navier-Stokes equations on a structured grid arising on a triangular domain. This mesh is obtained by applying to the initial triangle a number ℓ of refinement levels, in the way that each refinement step consists of splitting each triangle of the grid into four triangles by connecting the midpoints of its edges. In such grid, a non-orthogonal coordinate system $\{\mathbf{e}_1, \mathbf{e}_2\}$ can be fixed considering the directions of two of the edges of the initial triangle, and according to the definition of this spatial basis, a certain type of numbering the grid-points that is very convenient for identifying the neighboring nodes can be defined. This point, coming from the structured character of the grid, allows an efficient implementation of the finite element method, which provides advantages regarding the memory consumption as well as in the speed of the computation. As we will see, a few stencils are enough to represent the discrete operators associated with the linear terms of our problem, since these are equal for all the interior nodes. Since quadratic finite elements are used to approximate the velocity vector, the unknowns are located at the vertices of the triangulation, as well as at the midpoints of the edges. Therefore, different equations and, consequently, different stencils are obtained depending on the location of the grid-point. First, we will focus on the construction of the stencils associated with a vertex of the triangulation. We denote such node as $\mathbf{x}_{n,m}$, which is the center of a hexagon H composed of six congruent triangles, which form the support of the corresponding basis function. Thus, all the unknowns located at points of this hexagon can contribute to the stencils corresponding to the node $\mathbf{x}_{n,m}$. This fact implies that we are going to work with $(5\times5)-$stencils, see Figure 1. For the computation of these stencils, we extend the philosophy presented in [6] to the case of quadratic finite element methods. The strategy presented in such paper consists of using a reference hexagon, $\widehat{H}$, centered at $\widehat{\mathbf{x}}_{0,0} = (0,0)$, and with vertices $\widehat{\mathbf{x}}_{1,0} = (1,0)$, $\widehat{\mathbf{x}}_{1,1} = (1,1)$, $\widehat{\mathbf{x}}_{0,1} = (0,1)$, $\widehat{\mathbf{x}}_{-1,0} = (-1,0)$, $\widehat{\mathbf{x}}_{-1,-1} = (-1,-1)$ and $\widehat{\mathbf{x}}_{0,-1} = (0,-1)$. By considering the affine transformation mapping hexagon $\widehat{H}$ onto the arbitrary hexagon on which we wish to compute the stencil, the degrees of freedom and basis functions on $\widehat{H}$ can be translated to degrees of freedom and basis functions on the arbitrary hexagon. In this way, we can obtain an expression of the desired stencil as a function of certain stencils computed "a-priori" on the reference hexagon. The application of this strategy to quadratic finite elements

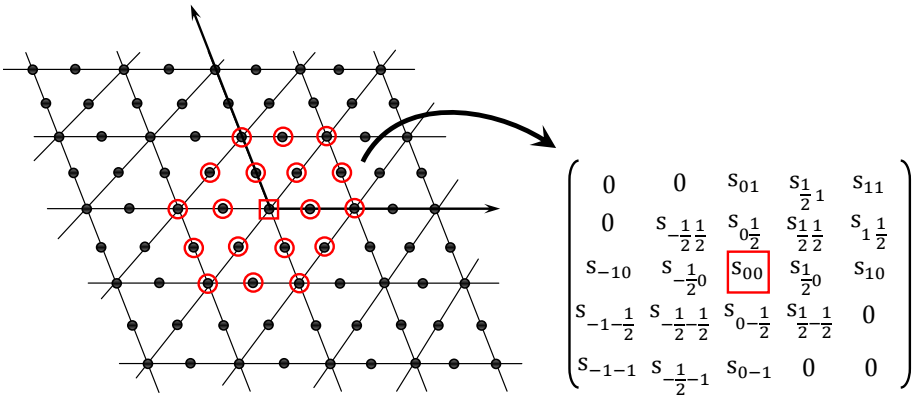

FIGURE 1. Stencil corresponding to a vertex interior to the grid.

becomes easy, since the affine transformation F_H that we have to use is the standard one commonly used in the assembly process, that is, $F_H : \widehat{H} \to H$ such that $\mathbf{x} = F_H(\widehat{\mathbf{x}}) = B_H\widehat{\mathbf{x}} + b_H$, with

$$B_H = \begin{pmatrix} x_{n+1,m} - x_{n,m} & x_{n+1,m+1} - x_{n+1,m} \\ y_{n+1,m} - y_{n,m} & y_{n+1,m+1} - y_{n+1,m} \end{pmatrix}, \quad b_H = \begin{pmatrix} x_{n,m} \\ y_{n,m} \end{pmatrix},$$

where $(x_{n+k,m+l}, y_{n+k,m+l})$ are the coordinates of $\mathbf{x}_{n+k,m+l}$. Therefore, $F_H(\widehat{\mathbf{x}}_{k,l}) = \mathbf{x}_{n+k,m+l}$ is satisfied, for the vertices, as well as for the midpoints of the edges, see Figure 2. After some computations analogous to those in [6], we can obtain expres-

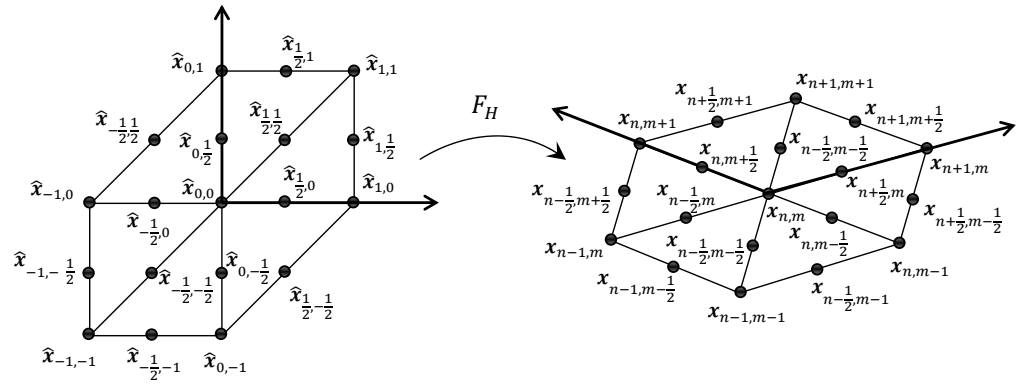

FIGURE 2. Reference hexagon and corresponding affine transformation F_H.

sions for the discrete operators involved in our problem. Regarding the Laplace operator, $S^v_{\Delta,\ell}$, where ℓ is the number of refinement levels applied to obtain the considered regular triangular grid, and v denotes that this operator is applied at the vertices of the grid, we obtain the following expression

$$S^v_{\Delta,\ell} = |\det B_H|(c^H_{11}\widehat{S}^v_{xx} + 2c^H_{12}\widehat{S}^v_{xy} + c^H_{22}\widehat{S}^v_{yy}),$$

where coefficients c^H_{ij} are the elements of the matrix $C_H = B_H^{-1}(B_H^{-1})^t$, and $\widehat{S}^v_{xx}$, $\widehat{S}^v_{xy}$ and $\widehat{S}^v_{yy}$ are the stencils computed on the reference hexagon, associated with

operators $-\partial_{xx}$, $-\partial_{xy}$ and $-\partial_{yy}$, respectively. These reference stencils are given in Figure 3, where the nodes involved in the stencil are surrounded by a circle, and the contribution of each node to the stencil is also given.

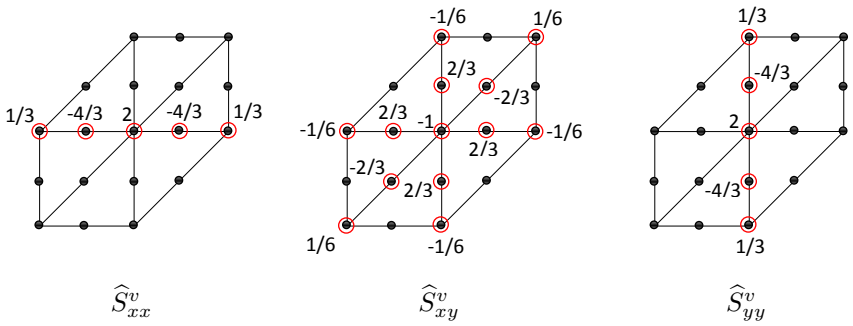

$\widehat{S}^v_{xx}$ $\widehat{S}^v_{xy}$ $\widehat{S}^v_{yy}$

FIGURE 3. Stencils computed on the reference hexagon, $\widehat{S}^v_{xx}$, $\widehat{S}^v_{xy}$ and $\widehat{S}^v_{yy}$, associated with operators $-\partial_{xx}$, $-\partial_{xy}$ and $-\partial_{yy}$ applied at the vertices of the triangulation.

Analogously, we can obtain the following counterpart expressions for the nodes located at the midpoints of the edges

$$S^m_{\Delta,\ell} = |\det B_H|(c^H_{11}\widehat{S}^m_{xx} + 2c^H_{12}\widehat{S}^m_{xy} + c^H_{22}\widehat{S}^m_{yy}),$$

where $\widehat{S}^m_{xx}$, $\widehat{S}^m_{xy}$ and $\widehat{S}^m_{yy}$ are given in Figure 4, where we illustrate the application of these operators at the midpoints of the "horizontal" edges, that is, the edges in the direction of vector $\mathbf{e}_1$ of the spatial basis. The corresponding operators at the "vertical" edges (those in the direction of vector $\mathbf{e}_2$) and at "diagonal" edges (those in the remaining direction) are analogous.

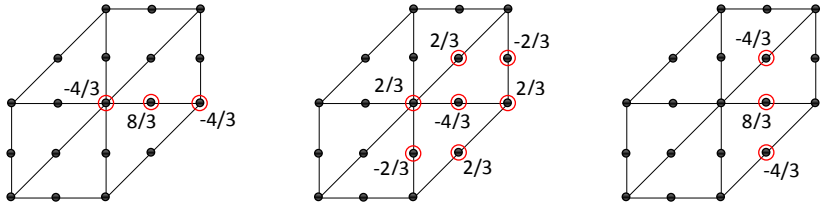

$\widehat{S}^m_{xx}$ $\widehat{S}^m_{xy}$ $\widehat{S}^m_{yy}$

FIGURE 4. Stencils computed on the reference hexagon, $\widehat{S}^m_{xx}$, $\widehat{S}^m_{xy}$ and $\widehat{S}^m_{yy}$, associated with operators $-\partial_{xx}$, $-\partial_{xy}$ and $-\partial_{yy}$ applied at the midpoints of the "horizontal" edges of the triangulation.

Following the same strategy, it is easy to get the stencil expressions of discrete operators appearing in the convective terms of the first equation. These terms correspond to first derivatives ∂_x and ∂_y, and again we must distinguish the application of these operators at the vertices of the triangulation or at the midpoints of the edges. We denote the discrete operators corresponding to these first derivatives as

$S^v_{\partial_x,\ell}$ and $S^v_{\partial_y,\ell}$ for the vertices, and $S^m_{\partial_x,\ell}$ and $S^m_{\partial_y,\ell}$ for the midpoints of the edges. Following the same procedure as previously explained for the Laplace operator, we can obtain the following expressions as a function of stencils computed in the reference hexagon:

$$\begin{aligned} S^v_{\partial_x,\ell} &= |\det B_H|(b^H_{11}\widehat{S}^v_x + b^H_{21}\widehat{S}^v_y), \\ S^v_{\partial_y,\ell} &= |\det B_H|(b^H_{12}\widehat{S}^v_x + b^H_{22}\widehat{S}^v_y), \\ S^m_{\partial_x,\ell} &= |\det B_H|(b^H_{11}\widehat{S}^m_x + b^H_{21}\widehat{S}^m_y), \\ S^m_{\partial_y,\ell} &= |\det B_H|(b^H_{12}\widehat{S}^m_x + b^H_{22}\widehat{S}^m_y), \end{aligned}$$

where the coefficients b^H_{ij} are the entries of matrix B_H^{-1}, and the corresponding reference stencils for ∂_x, that is, $\widehat{S}^v_x$ and $\widehat{S}^m_x$, are given in Figure 5. Note that again, for

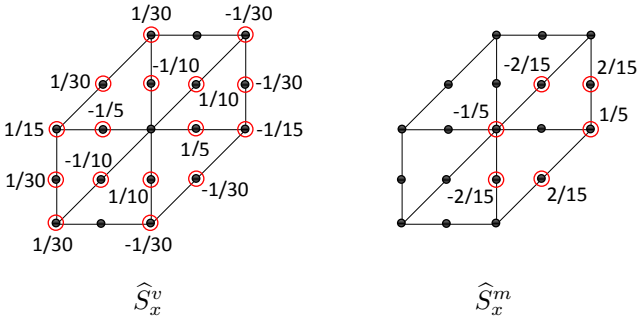

$\widehat{S}^v_x$ $\widehat{S}^m_x$

FIGURE 5. Stencils computed on the reference hexagon, $\widehat{S}^v_x$, and $\widehat{S}^m_x$, associated with operator ∂_x, involved in the convective terms, applied at the vertices and at the "horizontal" midpoints.

ease of presentation, in Figure 5, only the stencils corresponding to midpoints of the "horizontal" edges are displayed. However, analogously to the case of the Laplace operator which is illustrated in Figure 4, the stencils corresponding to vertical and diagonal edges are given by the same expressions but centered in such points.

Finally, we must deal with the stencils associated with the divergence operator of the velocity appearing in the second equation. Since this equation corresponds to the pressure unknown, which is discretized by linear finite elements, there will be only stencils associated with the vertices of the grid. Thus, denoting by $S^v_{\nabla_x,\ell}$ and $S^v_{\nabla_y,\ell}$ the operators corresponding to the first order derivatives appearing in the divergence operator, we can obtain their expressions as a function of reference stencils in the following way

$$\begin{aligned} S^v_{\nabla_x,\ell} &= |\det B_H|(b^H_{11}\widehat{S}^v_{\nabla_x} + b^H_{21}\widehat{S}^v_{\nabla_y}), \\ S^v_{\nabla_y,\ell} &= |\det B_H|(b^H_{12}\widehat{S}^v_{\nabla_x} + b^H_{22}\widehat{S}^v_{\nabla_y}), \end{aligned}$$

where the stencils corresponding to $\widehat{S}^v_{\nabla_x}$ and $\widehat{S}^v_{\nabla_y}$ are given as indicated in Figure 6.

Notice that this way of computing the stencil forms of the discrete operators as a function of the reference stencils is very efficient. This is due to the fact that each

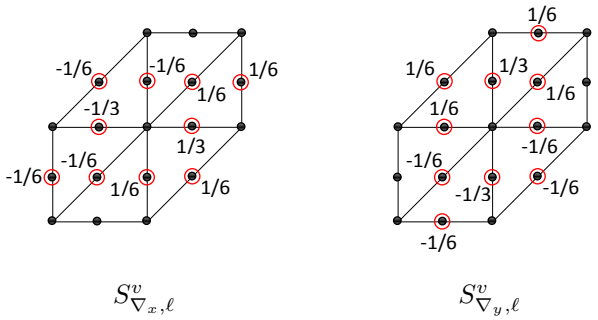

FIGURE 6. Stencils computed on the reference hexagon, $S^v_{\nabla_x,\ell}$ and $S^v_{\nabla_y,\ell}$ associated with the divergence of the velocity appearing in the second equation.

time that the stencil has to be computed, instead of assembling the contributions of the six triangles around the corresponding grid-point, we must simply multiply the coefficients obtained from the affine transformation by the stencils on the reference hexagon, which have been computed and stored a-priori.

3. Vanka smoother based multigrid method

It is well known that the performance of a multigrid method strongly depends on the choice of its components. In this section, the multigrid components considered in this work are presented. For the implementation of a geometric multigrid, first a hierarchy of grids must be defined. Here, we apply to the triangular domain several steps of a regular refinement process, which consists of dividing each triangle into four congruent triangles by connecting the midpoints of its edges. In this way, a nested hierarchy of regular grids is obtained, which is very appropriate for the application of a geometric multigrid method. Once the hierarchy of grids has been built, suitable discrete operators on each coarse grid have to be chosen for approximating the fine-grid discrete operator. Here, we use the direct discretization of the equations on each coarse grid, since it gives rise to reasonable approximations of the fine-grid discrete operator, ensuring the overall consistency of the discrete problem. The choice of inter-grid transfer operators is, of course, closely related to the chosen finite element. In this work, linear interpolation and its adjoint are chosen for the pressure unknown, since linear finite elements are used to approximate these unknowns. However, for the velocity unknowns, which are approximated by quadratic finite elements, the quadratic interpolation and its adjoint are preferred as inter-grid transfer operators. More concretely, in Figure 7, we show the coefficients involved in the restriction of each type of the grid-points in which the velocity unknowns are discretized. It is observed that for the midpoints of the horizontal, vertical and diagonal edges, the coefficients of the corresponding restriction operator are the same.

The smoother usually plays an important role in multigrid algorithms, above all in the geometric approach. Therefore, the choice of a suitable smoother is an important feature for the design of an efficient geometric multigrid method, and even it requires special attention when one works with systems of PDEs, since the smoother should smooth the error for all unknowns. Moreover, for the problem we are dealing with, an additional difficulty appears, since it results in a system

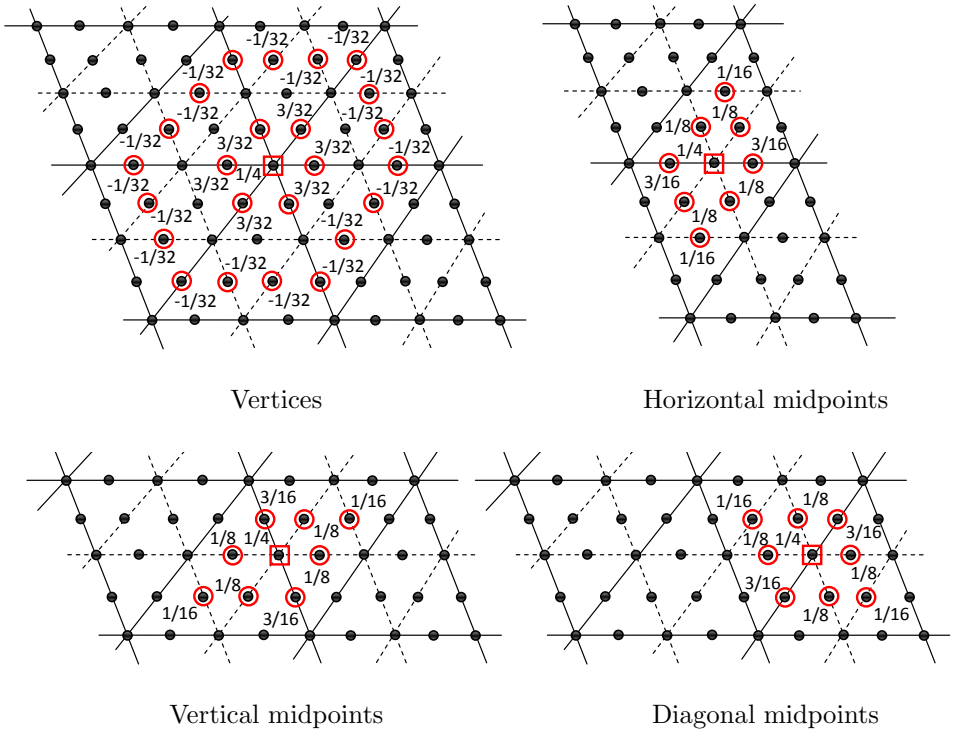

FIGURE 7. Restriction for the different types of grid-points where velocity unknowns are located.

of saddle point type [1], with a zero block diagonal which renders impossible the application of a collective point-wise relaxation. An overview of multigrid methods for discretizations on rectangular grids of this type of problems is presented in [13], where coupled or box-relaxation and decoupled distributive relaxation methods appear as the most suitable for this kind of problems. Due to the fact that for some systems of equations it is a challenge to design an efficient distributive relaxation scheme, box-relaxation seems to be the best option. This is performed by decomposing the mesh into small subdomains and treating them separately in a coupled form, that is, all the equations corresponding to the points in each subdomain are solved simultaneously as a system. This class of smoothers was introduced by Vanka [19] to solve the finite difference discretization on rectangular grids of the Navier-Stokes equations. Since then, much literature can be found about the application of this type of smoothers, mainly in the field of Computational Fluid Dynamics (CFD) [9, 10, 18]. These smoothers have been mainly applied on rectangular grids, but here we present an extension of box-smoothers to triangular grids, suitable for the Navier-Stokes equations. In particular, for each vertex of the grid, the unknowns that we simultaneously solve are the pressure unknown located at this vertex and the 38 velocity unknowns located at the hexagon around such vertex, as we can see in Figure 8. Thus, the proposed smoother consists of visiting the vertices of the grid in a lexicographic ordering and, for each vertex, solving the resulting $(39 \times 39)-$system corresponding to the box associated with that point. This type of smoother turns out to be very costly, but it is necessary for the good behavior of the multigrid method for our problem. A cheaper variant of this class of

smoothers is the diagonal point-wise box Gauss-Seidel, which will be investigated in the future.

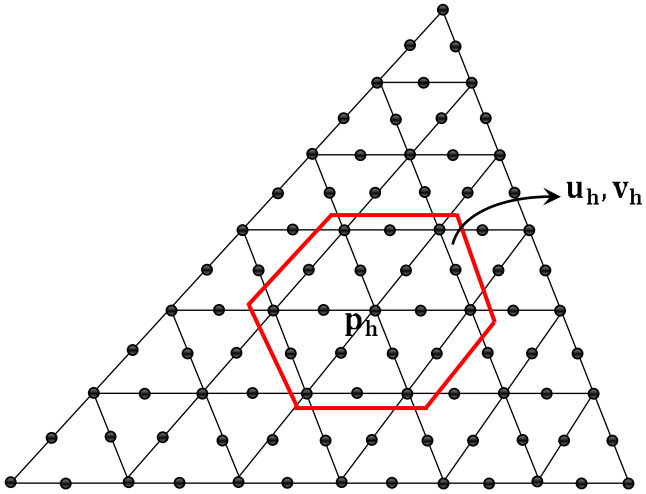

FIGURE 8. Unknowns simultaneously updated in point-wise box Gauss-Seidel smoother.

4. Numerical experiments: Triangular cavity problem

This section deals with the multigrid solution of the problem of steady incompressible viscous flow within a driven triangular cavity discretized by P2-P1 finite elements. Steady recirculating flow is of primary importance in computational fluid dynamics, see [12, 15] and references therein. The most investigated case in the literature is the cavity flow problem, in which a viscous fluid is enclosed by solid motionless boundaries except for a translating segment which drives the recirculation through shear stress. By far the most widely studied cavity flow problem is that consisting of a two-dimensional square enclosure with one side translating with uniform velocity, [7, 16]. Indeed, due to the simplicity of the geometry and boundary conditions, it has become an important benchmark problem for testing new computational algorithms. Fewer numerical studies of flow in non-rectangular cavities have been carried out, [5, 12, 14, 20], despite their wide range of applications, in which sharp corners are common. In this way, the problem under consideration is that of steady two-dimensional flow in a solid walled triangular cavity, driven by the uniform shearing motion of the upper side wall, [11, 15]. The boundary conditions are no slip on sides of the triangle moving with a velocity of constant magnitude, and on fixed sides the velocity is zero. This problem is solved on two triangular domains with different geometries. In both cases a target fine grid has been obtained by applying eight refinement levels. The first domain consists of a unit equilateral triangle, as shown in Figure 9 (a), together with the boundary conditions previously specified. The Reynolds number considered for the simulation is Re=20. In Figure 9 (b), the streamtraces in the flowfield are shown together with the velocity vectors. It is observed that a large central eddy covers most of the cavity, except a small zone close to one vertex of the cavity, in which a small recirculating eddy appears. This simulation has been done using the multigrid method

proposed on each iteration of the fixed point method. An F-cycle with three pre- and three post-smoothing steps has been considered, giving rise to a very efficient algorithm which achieves convergence factors close to 0.1. On the other hand, the

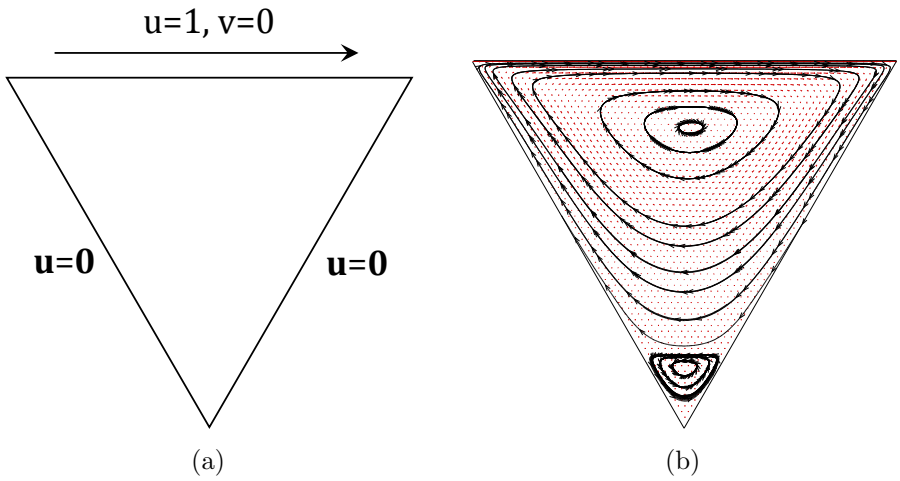

FIGURE 9. (a) Geometry and boundary conditions for the equilateral triangular cavity problem. (b) Streamtraces and velocity vectors for the problem in the equilateral triangular domain, for Reynolds number Re=20.

second test consists of solving the steady viscous flow problem in an isosceles triangular cavity, characterized by a very small angle. More concretely, the domain of the second experiment is an isosceles triangle with base angle of 75^{O}, as depicted in Figure 10 (a). The solution is shown in Figure 10 (b), where we can observe that four eddies appear instead of the pair of eddies observed in the first test case, for the equilateral triangular domain. However, regarding the efficiency of the multigrid method, a slight deterioration of the convergence factor is suffered due to the anisotropy of the grid. In particular, a convergence factor about 0.2 is obtained. To overcome this difficulty, line box-smoothers are required, but this will be considered in future work.

References

[1] M. Benzi, G.H. Golub and J. Liesen, Numerical solution of saddle point problems, Acta Numerica, 14: 1–137, 2005. Cambridge University Press, United Kingdom.
[2] A. Brandt, Multigrid techniques: 1984 guide with applications to fluid dynamics, GMD-Studie Nr. 85, Sankt Augustin, Germany, 1984.
[3] F. Brezzi and M. Fortin, Mixed and Hybrid Finite Element Methods. Springer-Verlag, New York, 1991.
[4] W. Briggs, V.E. Henson, S. McCormick, A Multigrid Tutorial, Society for Industrial and Applied Mathematics, 2000.
[5] J.H. Darr, S.P. Vanka, Separated flow in a driven trapezoidal cavity, Phys. Fluids, 3: 385–392, 1991.
[6] F.J. Gaspar, J.L. Gracia, F.J. Lisbona, C. Rodrigo, Efficient geometric multigrid implementation for triangular grids, Journal of Computational and Applied Mathematics, 234: 1027–1035, 2010.
[7] U. Ghia, K.N. Ghia, C.T. Shin, High-Re solutions for incompressible flows using the Navier-Stokes equations and a multigrid method, J. Comput. Phys., 48: 387–411, 1982.
[8] W. Hackbusch, Multi-grid methods and applications, Springer, Berlin, 1985.

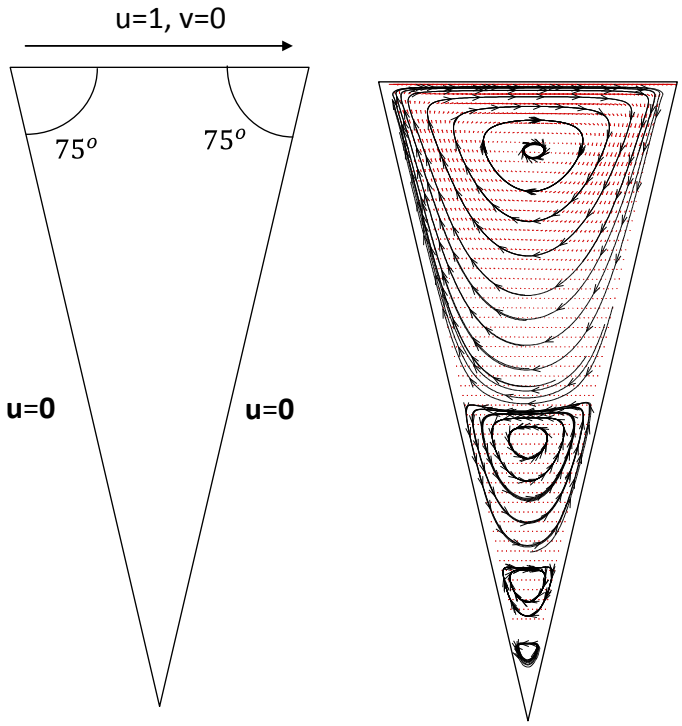

FIGURE 10. (a) Geometry and boundary conditions for the isosceles triangular cavity problem. (b) Streamtraces and velocity vectors for the problem in the isosceles triangular domain, for Reynolds number Re=20.

[9] V. John, A comparison of parallel solvers for the incompressible Navier-Stokes equations, Comput. Visual. Sci., 1: 193–200, 1999.
[10] V. John, L. Tobiska, Numerical performance of smoothers in coupled multigrid methods for the parallel solution of the incompressible Navier-Stokes equations, Int. J. Numer. Meth. Fluids, 33: 453–473, 2000.
[11] R. Jyotsna, S.P. Vanka, Multigrid calculation of steady, viscous flow in a triangular cavity, J. Comput. Phys., 122: 107–117, 1995.
[12] W.D. McQuain, C.J. Ribbens, C.-Y. Wang, L.T. Watson, Steady viscous flow in a trapezoidal cavity, Computers and Fluids, 23: 613–626, 1994.
[13] C.W. Oosterlee, F.J. Gaspar, Multigrid relaxation methods for systems of saddle point type, Appl. Numer. Math., 58: 1933–1950, 2008.
[14] C.J. Ribbens, C.-Y. Wang, L.T. Watson, K.A. Alexander, Vorticity induced by a moving elliptic belt, Computers and Fluids, 20: 111–119, 1991.
[15] C.J. Ribbens, L.T. Watson, C.-Y. Wang, Steady viscous flow in a triangular cavity, J. Comput. Phys., 112: 173–181, 1994.
[16] R. Schreiber, H.B. Keller, Driven cavity flows by efficient numerical techniques, J. Comput. Phys. 49: 310–333, 1983.
[17] U. Trottenberg, C.W. Oosterlee, A. Schüller, Multigrid Academic Press, New York, 2001.
[18] S. Turek, Efficient solvers for incompressible flow problems: an algorithmic and computational approach, Springer, Berlin, 1999.
[19] S.P. Vanka, Block-implicit multigrid solution of Navier-Stokes equations in primitive variables, Journal of Computational Physics, 65: 138–158, 1986.
[20] M. Vynnycky, S. Kimura, An investigation of recirculating flow in a driven cavity, Phys. Fluids, 6: 3610–3620, 1994.

IUMA, Department of Applied Mathematics, University of Zaragoza, Spain
E-mail: fjgaspar@unizar.es and carmenr@unizar.es
URL: http://www.unizar.es/pde/fjgaspar/index.html

Departamento de Ingeniería Mecánica, Escuela Superior Técnica; Instituto de Investigaciones Científicas y Técnicas para la Defensa, Villa Martelli, Buenos Aires, Argentina
E-mail: elvioh@citefa.gov.ar